



**Manchester
Metropolitan
University**

Allen, NS, Hamzah, H, Edge, M, Liauw, CM, Catalina, F, Edge, R and Navaratnam, S (2018) Photochemistry and photopolymerisation of substituted 2-methylantraquinones and novel 2-acryloxymethylantraquinone in radiation curing. *Journal of Photochemistry and Photobiology A: Chemistry*, 356. pp. 530-544. ISSN 1010-6030

Downloaded from: <https://e-space.mmu.ac.uk/620711/>

Publisher: Elsevier

DOI: <https://doi.org/10.1016/j.jphotochem.2018.01.006>

Usage rights: Creative Commons: Attribution-Noncommercial-No Derivative Works 4.0

Please cite the published version

<https://e-space.mmu.ac.uk>

PHOTOCHEMISTRY AND PHOTOPOLYMERISATION OF SUBSTITUTED 2-METHYLANTHRAQUINONES AND NOVEL 2-ACRYLOXYMETHYLANTHRAQUINONE IN RADIATION CURING

Norman S. Allen*, Hazira Hamzah, Michele Edge and Chris. M. Liauw
Chemistry and Environmental Sciences Department
Faculty of Science and Engineering
The Manchester Metropolitan University
Chester Street, Manchester M1 5GD, UK

Fernando Catalina
Departamento de Quimica Macromolecular Aplicada
Instituto de Ciencia y Tecnologia de Polimeros (CSIC)
C/Juan De La Cierva, 3, 28006, Madrid, Spain
(Fcatalina@ictp.csic.es)

Ruth Edge
Dalton Cumbrian Facility
University of Manchester, West lake Science and Technology Park, Moor Row, Whitehaven, CA24 3HA, UK
(Ruth.edge@manchester.ac.uk)

Suppiah Navaratnam
Biomedical Sciences Research Institute, University of Salford, Manchester, UK
(e-mail: navaratnam1000@gmail.com)

*Contact: Norman.Allen@sky.com (Emeritus Professor)

Keywords: Photochemistry; Photopolymerisation; 2-Methylantraquinones; flash photolysis; laser photolysis.

ABSTRACT

Anthraquinones have been the subject of numerous photochemical studies and their photopolymerization activities have been examined under various conditions to improve more efficient photochemical systems. This article involves further detailed investigations into the photophysical, photochemistry and photopolymerisation properties of 4 commercial derivatives of 2-substituted anthraquinone, namely, 2-Bromomethylantraquinone (2BA), 2 Chloromethylantraquinone (2CA), 2 Ethylantraquinone (2EA), 2 Hydroxymethylantraquinone (2HA) and one novel synthesized anthraquinone, 2 Acryloxymethylantraquinone (2AA). 2AA is synthesized from 2HA. The results from both spectroscopic and analysis studies proved the 2AA to having the ester link. Absorption spectroscopy and solvent shift data are used to characterise their spectral activity. Luminescence studies involving fluorescence and phosphorescence analysis indicates efficient intersystem crossing to triplet state and $n-\pi^*$ nature of the lowest excited triplet state. The polymerisation activity was studied using methyl methacrylate (MMA) and analysis of the cure rate was measured using the gravimetric method. All the compounds are shown to be highly dependent on the structure. However, the rate of polymerisation (R_p) was reduced in the presence of amine. This is consistent with other results, proving the behaviour of derivatives with $n-\pi^*$ configuration. Hardness tests for all compounds took place using a different formula of acrylated resin/monomer systems. The excited state characteristics of the methyl derivatives have also been examined using micro and nanosecond flash photolysis. Triplet absorption spectra of all the anthraquinone derivatives show a significant red shift in the region of 340-370nm with increasing solvent polarity due to stabilisation of the lowest triplet state by solvent reorganization. Hydrogen atom abstraction takes place in 2 propanol, forming a semiquinone radical. In the presence of the tertiary amine, triethylamine, all

anthraquinone derivatives show the formation of intermediary species related to either the exciplex or the radical ion pair. Under aerobic conditions, the first decay rate for all anthraquinone derivatives increases and showed oxygen to be a good quencher with a bimolecular rate constant of around $2 \times 10^8 \text{ mol.dm}^{-3} \text{ s}^{-1}$. Relative to benzophenone, the molar absorption coefficient, ϵ , and quantum yield of intersystem crossing, Φ_{isc} were calculated, and it is summarised that the value for Φ_{isc} for all compound is less than 1.00 and controls to a major extent their photochemical activities.

INTRODUCTION

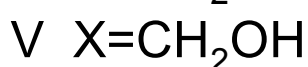
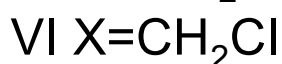
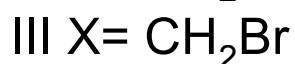
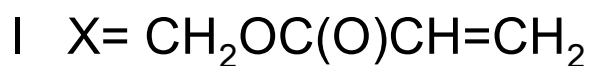
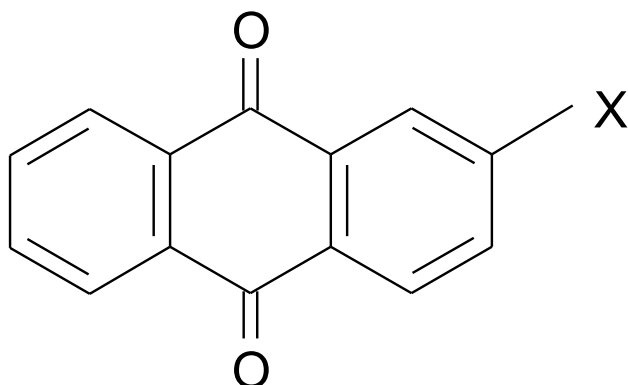
The photophysical and photochemical properties of anthraquinone derivatives has been one of the main areas of study in our research investigating the relationship and understanding between molecular structure, excited state properties and light stability and photochemical activity [1-8]. They have many applications in dye and pigment-based, water and oil miscible, acrylated matrices. One of our main targets in this respect has been as visible sensitizers for photocuring and photocrosslinking of resins and polymer materials. Much of the emphasis in this work has concentrated on various 2/3-substituted derivatives where from a photochemical point-of-view there is high activity compared with 1-substitution where excited state activity is strongly suppressed through intra-molecular interactions with the primary central aromatic carbonyl group [1,2].

Substitution in the 2-position on anthraquinone with electron withdrawing functionalities gives rise to often high photochemical reactivity through enhancing the reactivity of the lowest lying triplet $n\pi^*$ state while electron donating functionalities can enhance activity through simply increased absorption of the light energy in the visible region of the spectrum of excitation. Novel acryloxy and acrylamino and amido derivatives have been synthesised and produced significant enhancement in desirable photoinitiators for polymerisation and curing reactions whilst at the same time minimising unreacted diffusion in coatings systems. Direct halogenation has also given rise to high photochemical activity through photolysis giving aromatic and halogen free radicals through laser photolysis studies [6].

In an extension of our earlier studies we have investigated here the photochemical excited state properties and photopolymerisation activity of a range of 2-substituted methylantraquinones using the methylene group as a spacer. Here the role of 2-bromo-(2BA), 2-chloro-(2CA), 2-ethyl(2EA), 2-hydroxy-(2HA) and 2-acryloxy (methylantraquinone) derivatives have been investigated. No studies have been undertaken on these derivatives previously and indeed the 2-acryloxymethyl (2AA) derivative is synthesised here for the first time. Structure I illustrate the compounds investigated. Absorption, luminescence and micro- and nano-second flash studies are presented coupled with detailed excited state and intersystem crossing reaction rates.

Structures I

STRUCTURES



EXPERIMENTAL

Materials

High purity 2BA, 2HA, 2CA and 2HA derivatives, FENBID, quinine bisulphate monohydrate, triethylamine, methyl methacrylate (MMA) and benzophenone, were obtained from Sigma/Aldrich Chemicals (Poole, UK), and used as received. All organic solvents were of high purity solvent grade obtained from Romil Chemicals Ltd (Cambridge, UK). TPGDA (Tripropylene Glycol Diacrylate) and GPTA (Glycerol Propoxylate Triacrylate) commercial photopolymerisable acrylate resins were obtained from Akcros Chemicals, Manchester, UK.

Synthesis of 2-acyloxymethylantraquinone

In this study 2HA (1g, 0.0042 mol) was dissolved in propylene oxide (150 ml). A solution of acryloyl chloride (0.68 ml, 0.0084 mol) was dissolved in 20 ml of propylene oxide and was then added dropwise to the anthraquinone over a period of 20 minutes. The solution was left stirring at 0°C for 20 minutes followed by the addition of 0.58 ml of triethylamine (0.0042 mol). The solution was then warmed to 40°C and left stirring for 5 hrs and then overnight for 14 hrs at room temperature. The solution was then precipitated in water giving a yellow precipitate which was washed in water and recrystallised in ethanol followed by drying in a vacuum (mp. 215°C).

The FTIR analysis confirmed the identity of the 2AA derivative broadband at $\sim 3400\text{cm}^{-1}$ is the O-H stretch. This band appears in combination with a hydrogen-bonded OH peak when alcohol is present in the reaction. An absorption frequency at 2900cm^{-1} to 2800cm^{-1} in both compounds is usually due to CH stretching. The frequency at which the C-H absorption occurs indicates the type of carbon to which hydrogen is attached. C-H stretching also appears at lower frequency, normally at about 2850cm^{-1} and 2750cm^{-1} . The strong absorbance at about 2680cm^{-1} to 2600cm^{-1} is also due to CH stretching.

The acid chloride shows a very strong band for the C=O group that usually appears in the range of 1810cm^{-1} to 1775cm^{-1} for aliphatic acid chloride. Acid chloride and anhydrides are the most common functional groups that have a C=O peak appearing at such a high frequency.

In the novel anthraquinone spectrum, the C=O spectrum absorbance due to the acid chloride results in a novel 2-substituted anthraquinone with a C=O group attached to the compound. A medium strong absorption occurs at about 1675cm^{-1} which is unchanged before and after the reaction. This band suggested the presence of a quinone group. Literally the quinone group absorbs at 1660cm^{-1} . The C=C stretching bands for aromatic rings usually occur in pairs at 1600cm^{-1} and 1475cm^{-1} . These bands appeared in both spectra between 1630cm^{-1} – 1590cm^{-1} and 1475cm^{-1} . The band within the range 1400cm^{-1} to 1320cm^{-1} in the spectrum of the novel 2-substituted anthraquinone corresponds to methyl and methylene groups that are attached on the new compound. Substitution of 2-hydroxymethylanthraquinone to the carbonyl group on an acid chloride leads to the formation of an ester. Obviously in the spectrum peaks between 1300cm^{-1} – 1000cm^{-1} correspond to the presence of the ester group. The C-O stretching vibration of esters generally consists of two coupled asymmetric vibrations. The strong O – (C=O) absorption at 1150cm^{-1} to 1300cm^{-1} and the weaker C-O (C=O) are at 1500cm^{-1} to 1000cm^{-1} . The intense bands that appear between 900cm^{-1} to 700cm^{-1} are usually resulting from out of plane C-H bending vibrations from the aromatic ring. These bands are from strong coupling with adjacent hydrogen atoms and can also be used to assign the positions of substituents on the aromatic ring.

To elucidate the novel compound for the experiments, further H-NMR was also used to give information about the number of hydrogen nuclei (protons) as well as the nature of the immediate environment of each type. For this compound, the H-NMR spectrum showed signals attributed to hydrogens attached to aromatic ring with 4H singlets at $\sigma = 8.30$ and 3H singlets at $\sigma = 7.81$. The hydrogens attached to aromatic rings were easily identified and found in the region of 6.5 – 8.0 ppm. The high field signal at $\sigma = 5.37$ corresponded to the methylene group. The set of highly split doublets centred between $\sigma = 5.95$ - 6.55 were seen where the alkene hydrogens are expected. Other peaks were also seen for trans and cis coupling constants:

Rates of Photopolymerisation and Photocuring

Solutions of the anthraquinones ($2 \times 10^{-3}\text{M}$) in MMA monomer in ethyl acetate (50:50 v/v) were irradiated on an optical bench set-up utilising a 100 W high pressure Hg/W lamp (Phillips Laboratory Equipment, UK) at 10 cm distance using the full wavelength spectral output in a quart tube. Triethylamine was used at $2 \times 10^{-3}\text{M}$ and the

monomer was first treated with 2M sodium hydroxide solution to remove the inhibitor followed by drying overnight with anhydrous magnesium sulphate. Aliquots of the irradiated monomer were added to methanol and the precipitated PMMA polymer filtered off washed and dried and weighed. Rates of photopolymerisation were obtained from plots of percentage conversion vs irradiation time as described previously [9].

Sheen Pendulum Hardness

Hardness measurements were obtained using a Sheen pendulum hardness instrument (Sheen Ltd., UK). The surface hardness is measured by the ability of the film produced to dampen the oscillations of a swinging pendulum system through two 5 mm hemi-spheres resting on the film surface. Pendulum movement is monitored by an electronic impulse sensor and electronic counting device.

Spectroscopic Measurements

Absorption spectra were obtained using a Perkin-Elmer Lambda 7 absorption spectrometer and a Beckman DU7 spectrophotometer. Phosphorescence excitation and emission spectra were obtained using a Perkin-Elmer LS-50B luminescence spectrometer. Phosphorescence quantum yields were obtained in ethanol (absolute), ethanol:methanol (1:9 v/v) and diethyl ether:isooctane (1:2 v/v) at 77 K in liquid nitrogen using the relative method with benzophenone as a standard assuming a quantum yield of 0.74 in ethanol [12]. Clear glasses were obtained in all these solvents. All spectra were corrected using a Perkin-Elmer IBM compatible GEM package with an appropriate built-in correction factor for this purpose for the photoresponse of the photomultiplier and optics. Blank measurements were obtained on the solvents alone to correct for Raman scatter and subtracted from the original sample spectra. Phosphorescence lifetime measurements were obtained under the same condition (77K) using benzophenone as a standard for lifetime comparison (6.0 ms). Under this condition the influence of oxygen diffusion will be insignificant. Measurements were obtained via the GEM software and electronically gating the emission signal decay taking account of the phosphorescence lifetime and delay/gate widths in the data acquisition.

Time Resolved Absorption Spectroscopy Set-ups

End of pulse transient absorption spectra on the millisecond time scale were obtained using a kinetic flash photolysis apparatus equipped with two xenon filled flash lamps (operated at 10 kV) and a 150 W tungsten halogen monitoring source. Transient decay profiles were stored using a Gould model 1425 storage oscilloscope. Solutions were degassed using white spot nitrogen gas (<5 ppm O₂).

Laser flash photolysis. Laser flash photolysis experiments were carried out at the FRRF facility at Daresbury Laboratory using a Nd:YAG laser. The system essentially consists of a Q-switched

Nd:YAG (JK Lasers 2000 Series) laser capable of delivering up to 1 J of energy at 1064 nm in pulses of 12 ns duration as the excitation source. The fundamental beam can be frequency doubled, tripled and quadrupled to deliver light of 532, 355 and 266 nm, respectively. The harmonics are separated using a beam splitter. The sample under

investigation is contained in a quartz cell and replaced after each laser pulse using a remote-controlled flow system. The analysing beam generated by a xenon lamp, which can be pulsed to increase the analysing light up to 200 times in the UV region, passes through the sample at right angles to the laser beam. A shutter which opens a few microseconds before the laser pulse and closes again after the event under examination is completed, and appropriate filters are placed between the analysing lamp and sample to minimize the photolysis of the sample by the monitoring light. The monitoring light is then dispersed in wavelength by a monochromator and then onto a photodetector. The transmittance of light at this wavelength is detected by the photodetector before, during and after the laser pulse. The detector is also connected to an automatic back-off box which enables changes in transmittance to be observed by feeding back a signal equal and opposite to the detector anode current prior to the laser pulse, thus maintaining the anode current close to zero. The output of the photomultiplier (Hamamatsu R928) is displayed on a Tektronix TDS 380 digitizing oscilloscope. Data processing was performed on a Dan PC using software developed in house. Back-off and energy meter readings are digitized using an Analogue to Digital Converter (ADC) attached to a DI-AN data acquisition system. Data acquisition and processing are obtained by repeating the above procedure at successive wavelengths [9].

RESULTS AND DISCUSSION

Spectroscopic Study on the 2 Substituted methylantraquinones

The solvent usually has two main effects on the absorption spectra of molecules. The effects are shown as the absorption peaks becomes broader (*solvent broadening*) or the position of the λ_{\max} will differ in different solvents (*solvatochromic effect*). The effect of solvent on the absorption characteristics of the 2-substituted anthraquinones here was verified by UV-Vis absorption spectroscopy. Some interesting features have been observed regarding the nature of their absorption spectra and excited states.

In the present work, the absorption spectra of the five 2 substituted anthraquinones the (2BA), (2CA), (2EA), (2HA) and novel (2AA) were obtained in a series of solvents (cyclohexane, chloroform, dichloromethane, tetrahydrofuran, ethyl acetate, acetonitrile and 2-propanol) with increasing dielectric constant. Solvents of lower polarity were unsuitable in terms of the solubility of most of the compounds. Figure 1 shows the UV spectra for two different absorptions at two different wavelengths (short wavelength absorption and long wavelength absorption) for the 2-bromo derivative. The intensities of the band at the shorter wavelengths (250-270 nm) are strongest. Molar absorptivities at these peaks are large compare to the long wavelength peak (Table 1). Normally the large molar absorption is associated with a probable $\pi \rightarrow \pi^*$ transition. However, changing the solvents from non-polar to polar results in small variable red and blue shifts, and here the red shift can obviously be seen from cyclohexane to chloroform (Table 2). The results show that for this peak, the compounds have a $\pi \rightarrow \pi^*$ character but this is also influenced by the $n \rightarrow \pi^*$ transition. The shorter wavelength absorption is usually due to vibrational bands of the $S_0 \rightarrow S_2$ or $S_0 \rightarrow S_3$. Excitation to a higher unoccupied orbital occurs because at shorter wavelengths, the energy required for the excitation is high.

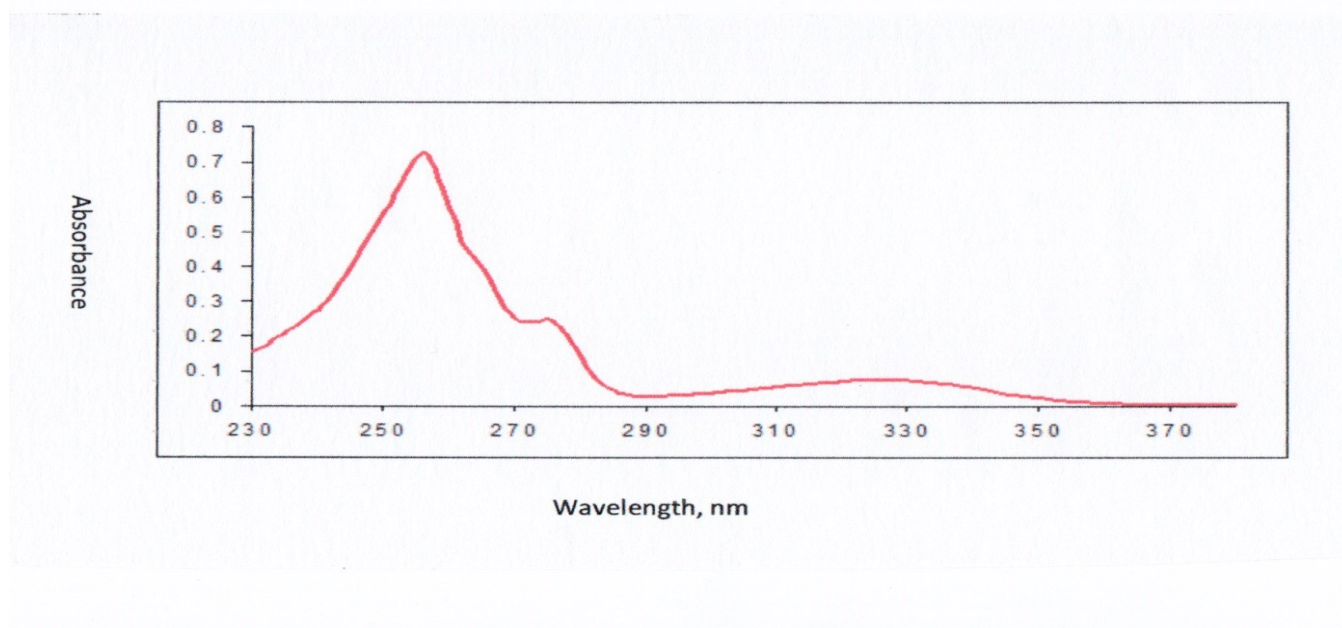


Figure 1: UV absorption Spectra For 2BA in dichloromethane showing absorption at short and long wavelength

It was cited in the literature that the absorption spectrum of anthraquinone consists of at least three $\pi \rightarrow \pi^*$ bands at 252 nm, 272 nm and 326 nm. The bands at 252 nm and 326 nm are assigned to the benzenoid chromophore and the 272 nm band to the quinoid chromophore. However, the bands of substituted anthraquinones shift to shorter or longer wavelengths according to the nature of the substituents. Examining the data in Tables 1 and 2, it is seen that there is only a slight difference in the absorption maxima and molar extinction coefficient data. The data is not much affected by solvent polarity. In previous literature, it was cited that 2-substituted anthraquinones do not exhibit large spectral shifts as they do not have a strong charge transfer interaction with the ring system. Therefore, this makes it less photochemically reactive. This fact is also in agreement with much of our previous reported studies [1-8]. We found that many 2-substituted anthraquinones exhibited a longest wavelength absorption maximum at between 330-360nm with a small and variable shift. For anthraquinone itself short wavelength absorptions are usually generated with $S\pi\pi^*$ transitions whereas the weaker absorption at long wavelengths is due to the $S_n\pi^*$ transition. Information as to understand the state of whether a molecule is in a $\pi\pi^*$ or an $n\pi^*$ state can often be obtained from the intensity, ϵ of the longest wavelength in the absorption spectrum. The low value of ϵ , mostly below 500 $\text{m}^2 \text{mol}^{-1}$ for most of the compounds shown in Table 2 suggests that the band represents an $n \rightarrow \pi^*$ transition and that the S_1 state is an ($n\pi^*$). Another confirmation to this conclusion can be made by changing the polarity of the solvent noting changes in the position of the band. Data for the long wavelength absorption maxima for most of the anthraquinone derivatives are red shifted from cyclohexane to chloroform. However, in the solvents of higher polarity, there is a small hypsochromic shift (blue shift) for most compounds where the position of the spectra had shifted to shorter wavelength with no notable change in the molar extinction coefficient. This variable small red and blue shift with

increasing solvent polarity is indicative of a strongly mixed $n\pi^*$ / $\pi\pi^*$ long wave transition. The small shift is also normally due to the rigid planar molecular structure of anthraquinone.

Table 1: Absorption Maxima (λ_{\max}/nm), Extinction Coefficients ($\epsilon/\text{mol}^{-1}\text{cm}^{-1}$) and Extinction Coefficients Logarithm ($\text{Log } \epsilon$) of 2AA, 2-CA and 2-EA For Long Wavelength Absorption Maxima in Different Solvents

Anthraquinone	2-Propanol			Acetonitrile			Ethyl Acetate			Tetrahydrofuran		
	λ_{\max}	ϵ	$\log \epsilon$	λ_{\max}	ϵ	$\log \epsilon$	λ_{\max}	ϵ	$\log \epsilon$	λ_{\max}	ϵ	$\log \epsilon$
(2BA)	330	10890	3.04	328	7530	2.88	328	6220	2.79	329	5700	2.76
(2CA)	326	4230	2.63	329	4910	2.69	330	5040	2.70	327	3520	2.55
(2EA)	329	2540	2.40	329	4360	2.64	330	11830	3.07	329	4050	2.61

Table 1 (cont.): Absorption Maxima (λ_{\max}/nm), Extinction Coefficients ($\epsilon/\text{mol}^{-1}\text{cm}^{-1}$) and Extinction Coefficients Logarithm ($\text{Log } \epsilon$) of 2BA, 2CA and 2EA For Long Wavelength Absorption Maxima in Different Solvents

Anthraquinone	Dichloromethane			Chloroform			Cyclohexane		
	λ_{\max}	ϵ	$\log \epsilon$	λ_{\max}	ϵ	$\log \epsilon$	λ_{\max}	ϵ	$\log \epsilon$
(2BA)	330	7000	2.85	332	10490	3.02	330	4950	2.69
(2CA)	327	3520	2.55	322	10600	3.02	324	5570	2.75
(2EA)	327	4120	2.61	307	8200	2.91	326	8640	2.94

Table 1 (cont.): Absorption Maxima (λ_{max} /nm), Extinction Coefficients ($\epsilon/\text{mol}^{-1} \text{cm}^{-1}$) and Extinction Coefficients Logarithm (Log ϵ) of 2HA and 2AA For Long Wavelength Absorption Maxima in Different Solvents

Anthraquinone	2-Propanol			Acetonitrile			Ethyl Acetate			Tetrahydrofuran		
	λ_{max}	ϵ	log ϵ	λ_{max}	ϵ	log ϵ	λ_{max}	ϵ	log ϵ	λ_{max}	ϵ	log ϵ
(2HA)	328	4590	2.66	330	4880	2.69	329	4330	2.64	327	2490	2.40
(2 AA)	327	3730	2.57	328	7230	2.86	324	11370	3.06	325	6870	2.84

Table 1 (cont.): Absorption Maxima (λ_{max} /nm), Extinction Coefficients ($\epsilon/\text{mol}^{-1} \text{cm}^{-1}$) and Extinction Coefficients Logarithm (Log ϵ) of 2HA and 2AA For Long Wavelength Absorption Maxima in Different Solvents

Anthraquinone	Dichloromethane			Chloroform			Cyclohexane		
	λ_{max}	ϵ	log ϵ	λ_{max}	ϵ	log ϵ	λ_{max}	ϵ	log ϵ
2HA	325	4520	2.66	329	69710	2.48	323	1490	2.17
2AA	327	3450	2.54	329	4790	2.95	321	4850	2.69

Table 2: Absorption Maxima (λ_{max} /nm), Extinction Coefficients ($\epsilon/\text{mol}^{-1} \text{cm}^{-1}$) and Extinction Coefficients Logarithm (Log ϵ) of 2BA, 2CA and 2EA For Short Wavelength Absorption Maxima in Different Solvents

Anthraquinone	2-Propanol			Acetonitrile			Ethyl Acetate			Tetrahydrofuran		
	λ_{max}	ϵ	log ϵ	λ_{max}	ϵ	log ϵ	λ_{max}	ϵ	log ϵ	λ_{max}	ϵ	log ϵ
(2BA)	256	95460	3.98	256	71850	3.86	262	57980	3,76	257	65750	3.82
(2CA)	255	42520	3.63	255	47940	3.68	253	68500	3.84	255	38870	3.59
(2EA)	256	35580	3.55	256	39520	3.60	259	67300	3.83	257	41270	3.62

Table 2 (cont.): Absorption Maxima (λ_{max} /nm), Extinction Coefficients ($\epsilon/\text{mol}^{-1} \text{cm}^{-1}$) and Extinction Coefficients Logarithm (Log ϵ) of 2BA, 2CA and 2EA For Short Wavelength Absorption Maxima in Different Solvents

Anthraquinone	Dichloromethane			Chloroform			Cyclohexane		
	λ_{max}	ϵ	log ϵ	λ_{max}	ϵ	log ϵ	λ_{max}	ϵ	log ϵ
(2BA)	259	66770	3.82	259	84380	3.92	256	49300	3.70
(2CA)	256	33280	3.52	257	38660	3.59	254	62220	3.79
(2EA)	258	39040	3.59	258	41320	3.62	256	78840	3.90

Table 2 (cont): Absorption Maxima (λ_{max} /nm), Extinction Coefficients ($\epsilon/\text{mol}^{-1} \text{ cm}^{-1}$) and Extinction Coefficients Logarithm (Log ϵ) of 2HA and 2AA for Short Wavelength Absorption Maxima in Different Solvents

Anthraquinone	2-Propanol			Acetonitrile			Ethyl Acetate			Tetrahydrofuran		
	λ_{max}	ϵ	log ϵ	λ_{max}	ϵ	log ϵ	λ_{max}	ϵ	log ϵ	λ_{max}	ϵ	log ϵ
2HA	256	42710	3.63	255	46460	3.67	257	60530	3.78	257	30850	3.49
2AA	254	50040	3.70	254	73290	3.87	258	47530	3.68	255	67550	3.83

Table 2 (cont): Absorption Maxima (λ_{max} /nm), Extinction Coefficients ($\epsilon/\text{mol}^{-1} \text{ cm}^{-1}$) and Extinction Coefficients Logarithm (Log ϵ) of 2HA and 2AA for Short Wavelength Absorption Maxima in Different Solvents

Anthraquinone	Dichloromethane			Chloroform			Cyclohexane		
	λ_{max}	ϵ	log ϵ	λ_{max}	ϵ	log ϵ	λ_{max}	ϵ	log ϵ
2HA	256	35680	3.55	257	44550	3.65	254	15910	3.20
2AA	256	28120	3.45	257	69710	3.84	253	50620	3.70

Luminescence Analysis

Fluorescence

The fluorescence emission maxima and quantum yield of all the 2-substituted anthraquinone derivatives are compared in Table 3. The data of all the compounds were recorded in four solvents of different polarity. The interactions between the excited state of the solute molecules with the surrounding solvent molecules may modify the quantum yield as well as the shape and spectral position of the emission bands. The emission wavelength maxima tend to undergo a hypsochromic shift (blue shift) from chloroform to acetonitrile, and most notable in acetonitrile for 2CA, 2EA and 2HA. There is not much difference in 2AA compared to the other commercial anthraquinones. This shift is normally associated with an $n\pi^*$ configuration of the lowest excited singlet states. All compounds exhibit low fluorescence quantum yields. This suggests a high rate of internal conversion to the ground state or intersystem crossing to the triplet state. Under El-Sayed 'selection rules' transitions of electron from $S_1(n,\pi^*)$ to the $T_n(n,\pi^*)$ is an "allowed transition". The energy gap between the two states is very small, therefore the rate constant for intersystem crossing from $S_1(n,\pi^*)$ to $T_n(n,\pi^*)$ is extremely fast thus giving out little fluorescence. The pattern observed from the data appeared to be similar to other aromatic carbonyls. In most aromatic carbonyl compounds, the intersystem crossing is very fast and often the compounds are non-fluorescent. The fluorescence absorption intensity that is exhibited by the excitation peak, and the emission spectral profile (curve) is often a mirror image (or nearly so) of the excitation curve, but shifted to longer wavelengths than the absorption as shown in Figure 2. This luminescence phenomenon happens for all compounds in the study indicating that the molecular structure in the ground and excited states remain unchanged.

Figure 2: Mirror Image of Absorption and Emission Spectra For a 2CA in chloroform

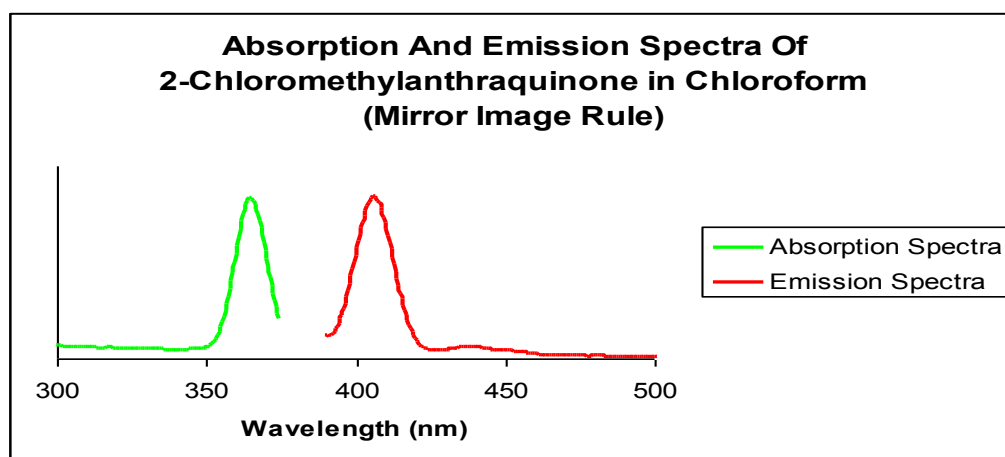


Table 3

Absorption (λ_{abs}),Fluorescence Emission (λ_{em}) and Quantum Yield (Φ_{F}) Data For 2-Substituted Anthraquinones In Different Solvent

Compound	Chloroform			Dichloromethane			Ethyl Acetate			Acetonitrile		
	λ_{abs}	λ_{em}	Φ_{F}	λ_{abs}	λ_{em}	Φ_{F}	λ_{abs}	λ_{em}	Φ_{F}	λ_{abs}	λ_{em}	Φ_{F}
2BA	332	410	1.5×10^{-2}	330	408	5.8×10^{-2}	328	409	2.0×10^{-3}	328	409	5.5×10^{-2}
2CA	322	410	4.5×10^{-2}	327	410	3.8×10^{-2}	327	409	4.3×10^{-3}	329	408	7.9×10^{-2}
2EA	325	411	3.1×10^{-2}	327	409	4.0×10^{-2}	330	410	6.0×10^{-3}	329	410	1.8×10^{-2}
2HA	329	413	4.3×10^{-2}	325	408	2.6×10^{-2}	329	409	3.8×10^{-2}	328	409	1.4×10^{-2}
2AA	329	413	1.7×10^{-4}	327	408	3.0×10^{-4}	328	414	4.3×10^{-4}	327	410	4.3×10^{-4}

Phosphorescence analysis

The phosphorescence emission data, quantum yields and triplet lifetimes for all derivatives are shown in the Table 4. The results exhibit relatively strong emission in ethanol for all anthraquinone derivatives. The phosphorescence quantum yield for 2BA and 2CA somehow is a little higher than other compounds, generally because of a heavy atom effect (Br, Cl) that significantly enhances the rate of intersystem crossing. However, the presence of heavy atoms reduces the phosphorescence lifetime of the T_1 state in 2BA and 2CA. The lack of fluorescence and strong phosphorescence quantum yields indicates that the lowest excited singlet and triplet states are $n\pi^*$ in character. As might be expected the 2-Br derivative exhibits a higher quantum yield than that for the 2-Cl derivative due to the heavy atom spin orbit coupling.

Table 4: Phosphorescence Properties of the 2-substituted methylantraquinones

	Ethanol		
	λ_{em}	Φ_p	τ / ms
2BA	459, 494, 536	0.301	1.67
2CA	459, 494, 534	0.246	1.96
2EA	459, 494, 536	0.194	2.34
2HA	459, 493, 536	0.225	2.04
2AA	459, 494, 536	0.232	2.10

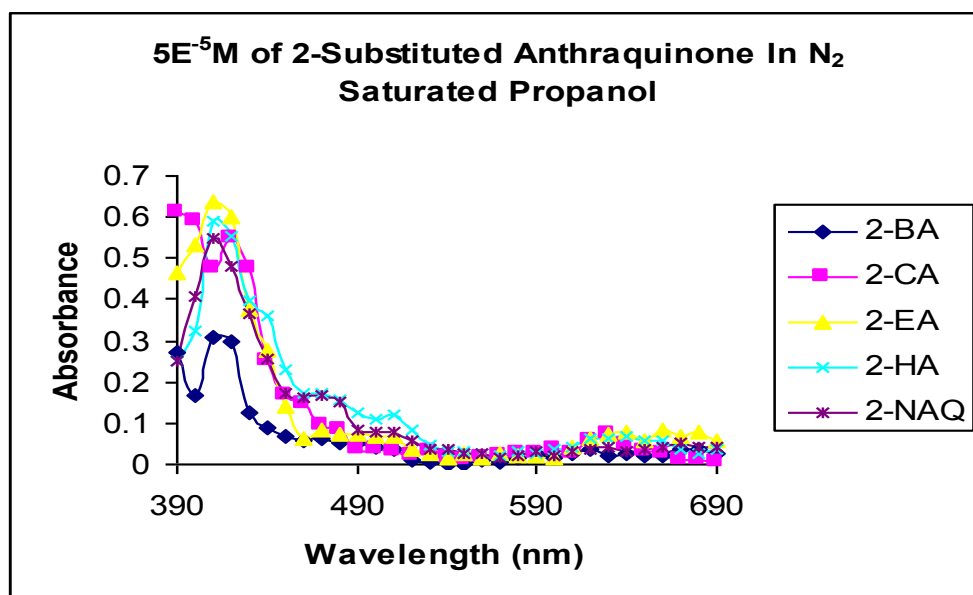
For all anthraquinone derivatives in this study, the singlet $n-\pi^*$ and $\pi-\pi^*$ levels are postulated to be very close. Therefore, vibronic coupling between almost degenerate $^1n-\pi^*$ and $^1\pi-\pi^*$ levels may lead to pseudo John-teller distortion of the lower state leading to enhance Frank-Condon factor (Frank-Condon factor becomes increasingly poor as the energy gap between two electronic states increases) [10]. Rapid deactivation of the lowest excited singlet states to the $^3n-\pi^*$ state happens via intersystem crossing. Fast intersystem crossing is strongly favoured by two factors: (i) the small size of the potential energy gap between the two states,

and (ii) the fact that crossings involves states of differing configuration. Phosphorescence emission occurs from an excited $^3n-\pi^*$ state to the ground state. This is strongly resembled in anthraquinone itself. Due to the vibronic coupling of the excited $^1n-\pi^*$ and $^1\pi-\pi^*$, the emission from a lower triplet $\pi\pi^*$ state was not observed.

Flash Photolysis (Microsecond)

End of pulse transient absorption spectra recorded for the 2-substituted anthraquinone compounds in N₂ saturated anaerobic 2-propanol are shown in Figure 3.

Figure 3: Microsecond flash spectra of 2-Substituted Anthraquinones in N₂ Saturated 2-Propanol

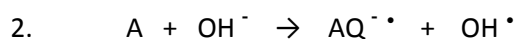


From the tabulated data it is seen that the addition of increasing the amounts of 2-propanol to acetonitrile solutions to all derivatives, increases the half-life of the triplet but reduces the kinetic order decay rate constants. The derivatives readily form a long lived radical by direct hydrogen atom abstraction from the 2-propanol donor molecule. The growth rate for all derivatives was taken at the same wavelength as the decay rate. This implies that the addition of 2-propanol to acetonitrile obviously produces the growth of another species. The first order growth rate constants of the transients observed are less than 100ns suggesting the formation of a radical ion pair [8].

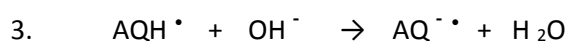
When triethylamine is added to all five compounds, the same trend happens. The half-life of the triplet is increased but the kinetic order decay rate constants reduced. The amine effect is evidence of the role of a longer species formed via electron transfer to give a radical anion via an exciplex. The activity of the transient species in the presence of this reductive solvent is shown in figure 4 as an example.



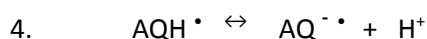
In the region between 460 - 490 nm, exists a very weak band. This band is normally weak in alcohol such as 2-propanol as seen in the above figure. However, the weak band can be enhanced in basic media. A radical anion is usually formed in two ways. Firstly, by electron transfer from the hydroxide or alkoxide to the excited triplet state of the anthraquinone.



Secondly the radical anion may also be formed from the semiquinone radical and hydroxyl anion to give water.



Both semianthraquinone radical and radical anion can also exist in equilibrium with each other by:



From these experiments, the compounds can be considered to potentially have medium or high photopolymerisation activity, similar to our previous work [6] on 2-bromoanthraquinone, 2-(1,1,1-trichloromethylanthraquinone), 2-(4-phenyl) triazoleanthraquinone and 2-methylcarboxyanthraquinone. This is also consistent with the relatively high triplet $\pi\pi^*$ activities of these molecules, indicating that they primarily operate via a mechanism of hydrogen atom abstraction. When a tertiary amine (10^{-3} M), triethylamine is added to the system, the most significant observation is an increase in absorbance in the region between 450 nm- 550 nm. A new absorption assigned to the anthraquinone radical anion is seen to appear in the above region. This effect is clearly illustrated in figure 4 as a typical example and Table 5 summarises the data of the compounds in the presence and absence of the tertiary amine.

Figure 4: End of pulse transient absorption spectra of 2-BA in absence and presence of triethylamine in nitrogen saturated 2-propanol solution.

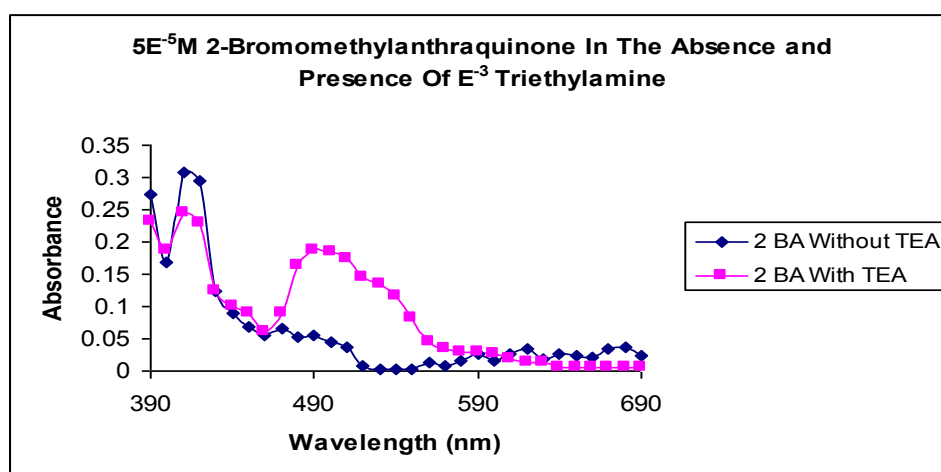


Table 5: End of Pulse Transient Absorption Data Produced on Microsecond Flash Photolysis of 2-Substituted Anthraquinone in Propanol with and without Triethylamine (10^{-3} M)

	TRANSIENT MAXIMA			
Anthraquinone	Semianthraquinone	Radical	Radical	Anion
	λ_{\max} (nm)	Absorbance	λ_{\max} (nm)	Absorbance
2-BA	410	0.308	-	-
2BA / TEA	410	0.245	490	0.186
2CA	420	0.55	-	-
2CA/ TEA	420	0.446	540	0.367
2 EA	410	0.637	-	-
2 EA / TEA	420	0.539	500	0.420
2 HA	410	0.591	-	-
2 HA / TEA	420	0.479	520	0.374
2 AA	410	0.55	-	-
2 AA / TEA	430	0.464	520	0.419

In addition to this, high absorbance values are observed with definite maxima for all the 2-substituted anthraquinone compounds around 400-420 nm even in the presence of an amine. This result correlates with previous results undertaken on 2-Acryloxyanthraquinone and 2-Acetoxyanthraquinone [8]. The high semiquinone absorbance values for all the compounds with and without the amine indicates that the compounds react predominantly via a hydrogen atom abstraction process. When an amine is present the compounds also show an absorption due to the radical anion; this also suggests the possibility of a dual reaction with electron transfer also occurring. In the presence of an amine there is a slight marked red-shift in the absorption wavelength maxima of both bands. However, it is interesting to note that all these anthraquinone compounds have low transient absorbance therefore making them potentially less photoactive.

Nano-second laser Flash Photolysis

Nanosecond laser flash photolysis study illustrates the difference in the activity of the lowest excited triplet states. The photopolymerisation activity of 2-substituted anthraquinone is associated with the ability of the molecule to undergo suitable photoreduction reactions which enable the production of long lived reactive species capable of initiating polymerisation.

Transient Behaviour in Acetonitrile

Transient absorption spectra of three of the 5 compounds of 2-substituted methylantraquinone derivatives in acetonitrile under anaerobic condition are shown in Figures 5 to 7. The transient absorptions are observed in the range of 320-600 nm and an average period of 250 to 500 ns and 1 to 2.5 μ s. The transients are compared at the equivalent absorbance of 0.5 or 1.0 at the laser excitation wavelength of 355nm. Generally, all the compounds exhibit single triplet absorptions with the maximum appearing in the lower end of the visible spectrum.

Figure 5

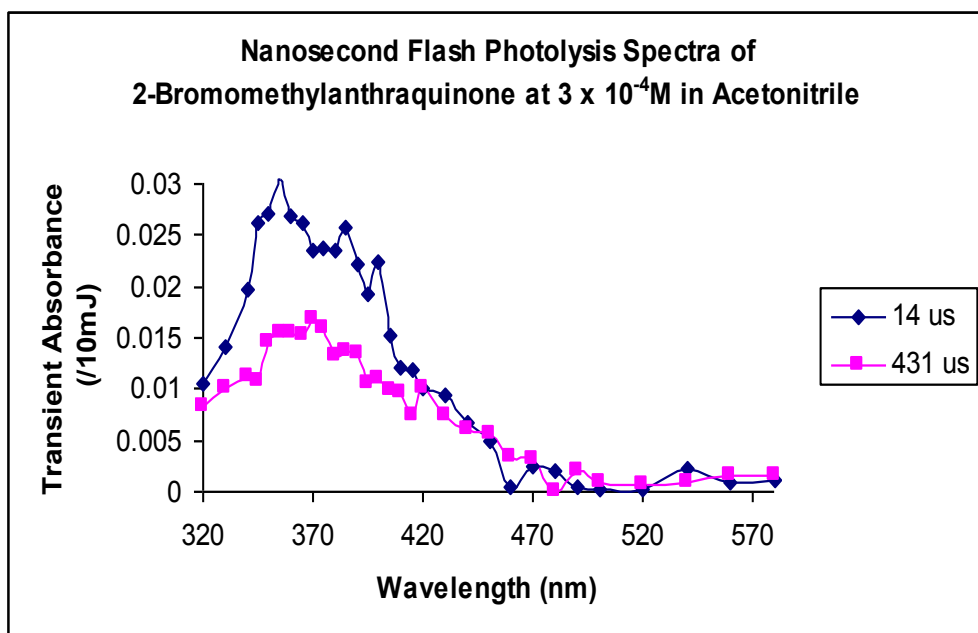


Figure:6

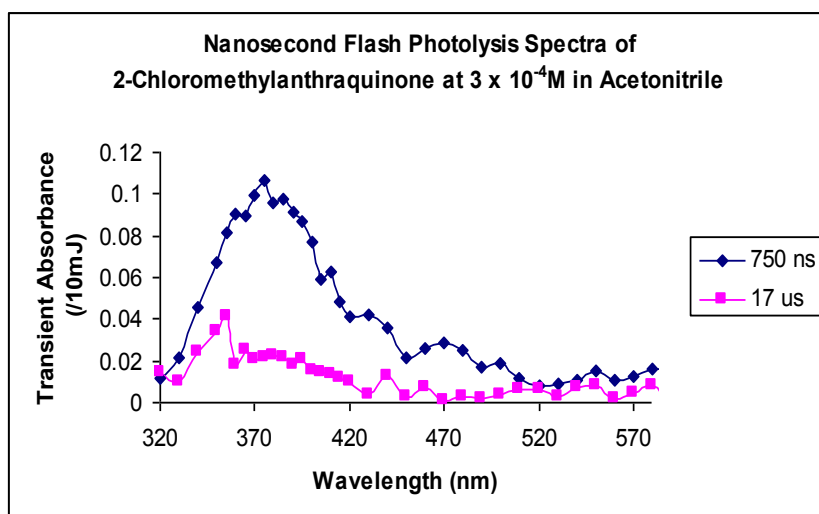
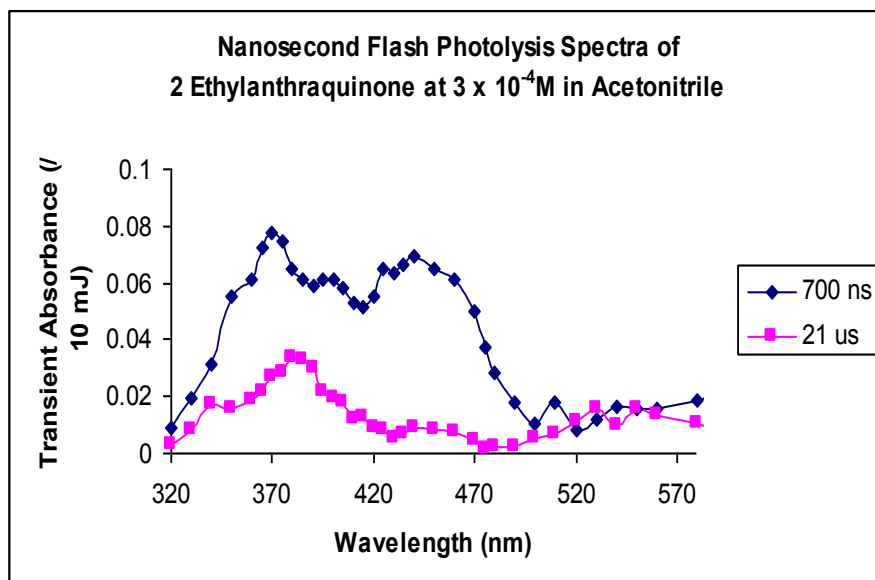


Figure: 7



It has been established from previous studies [8,11,12] that the nature of the triplet excited state according to the single triplet absorption maxima in the ranges 320-500 nm shown in nanosecond analysis, belongs to the triplet $^3n\pi$ state group. The new derivatives exhibited here also show similar spectra hence they also possess a triplet $^3n\pi$ state. Furthermore, the new derivative has an ester link in the 2-position, and it is apparent in many observations (8) that those compounds with an ester link in the 2-position have a triplet $^3n\pi$ excited state. Transient absorption spectra of all the anthraquinone derivatives were then measured in a hydrogen atom donating solvent 2-propanol to determine the reactivity of the triplet-triplet transient. Normally hydrogen atom abstraction by the carbonyl group is efficient when the T_1 state is ($n-\pi^*$).

Transient Behaviour in 2-Propanol

The influence of 2 –propanol can be seen from the results shown in Figures 8 to 11 for some of the compounds. The transient absorption spectra shown for all the 2-substituted anthraquinones showed a distinct difference between the behaviour shown for all anthraquinones in acetonitrile. The spectra seen are similar to those observed in the microsecond laser photolysis (Fig.3). It is clear that the triplet state of the anthraquinone derivatives studied have been quenched within the laser pulse by IPA to form the semiquinone radicals. Further increase in absorbance due to the radicals is also seen with times up to about ten microseconds.

Figure: 8

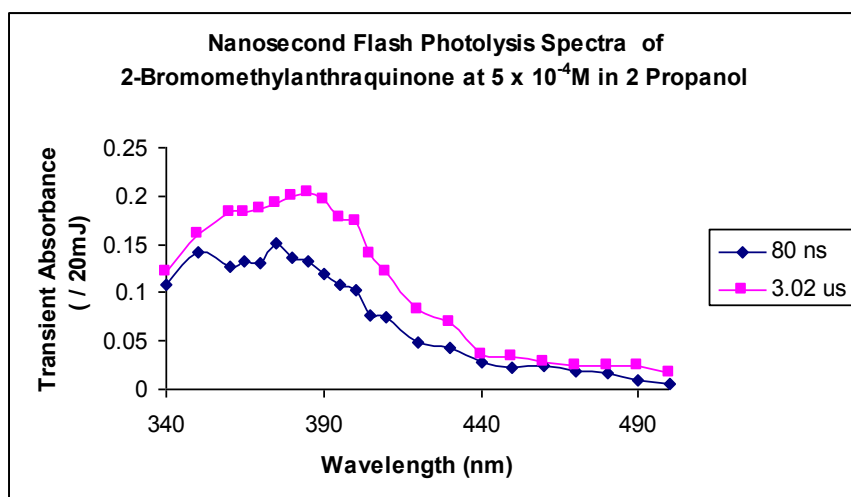


Figure: 9

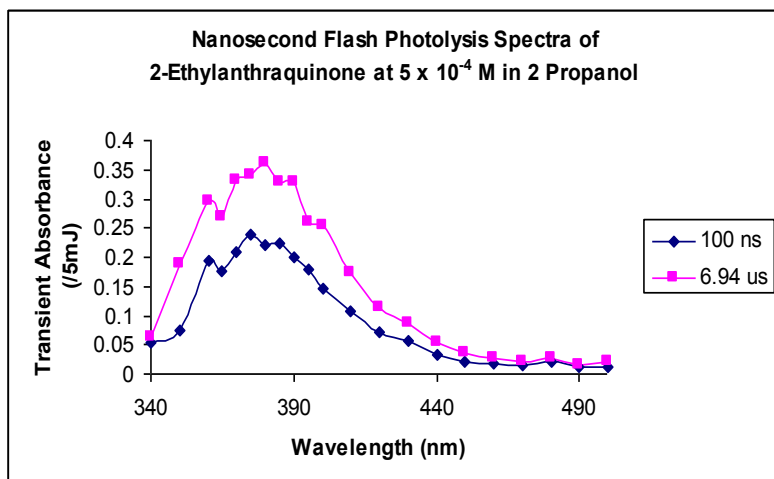


Figure: 10

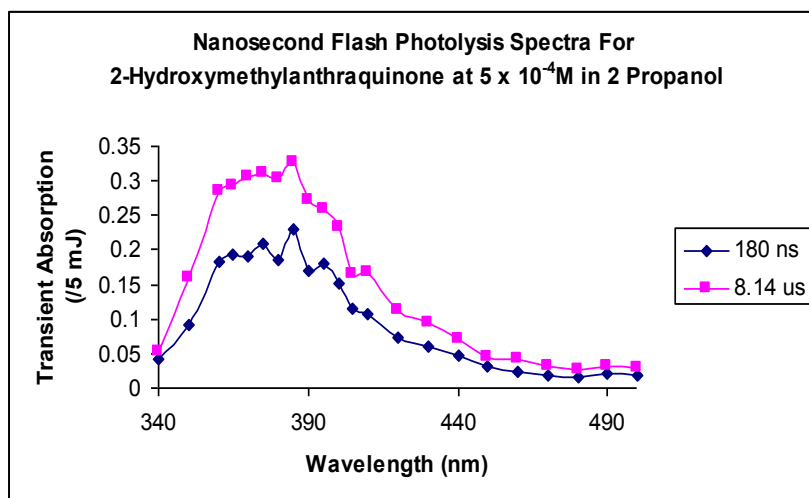
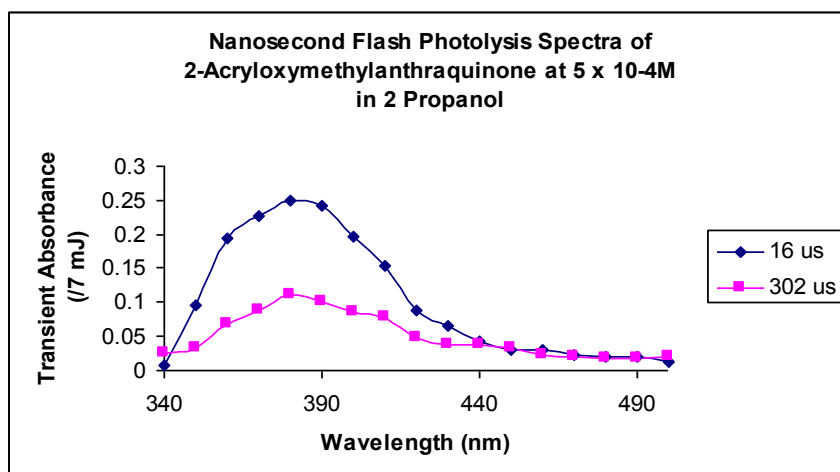
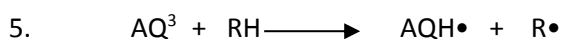


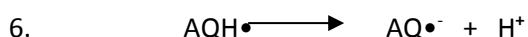
Figure: 11



Significantly in 2-propanol there is an increasing activity by the species with higher transient absorbances. This effect is attributed to the presence of a long lived transient due to the production of the semiquinone radical whereas in acetonitrile only the triplet-triplet formation and decay is observed. The triplet states of the parent anthraquinone abstract the hydrogen atom from the donor solvent, 2-propanol, producing the intermediate neutral semianthraquinone radical (AQH•)



In some hydroxylic solvents, such as 2-propanol, a neutral semianthraquinone radical is converted rapidly to a radical anion (AQ•⁻)



The presence of the radical anion is also well established [8,11,12]. Accordingly, the neutral semianthraquinone (AQH•) radical is short lived and the semianthraquinone radical anion (AQ•⁻) is stable and long lived. This finding is coherent with the activity observed by all the 2-substituted anthraquinones used in this study. It is interesting to note that the most long lived radical seen in this study exists in 2-acryloxymethylantraquinone, the novel 2-substituted anthraquinone which has an ester link. This is possibly due to de-esterification may take place at the ring position to give a long lived, stabilized aromatic radical. This reason is agreeable with the previous study on 2-methylcarboxyanthraquinone which also has an ester link and exhibits a long lived residual transient [8]. The photoactivity of the anthraquinones also depends on their triplet lifetimes. Triplet lifetimes of the anthraquinone derivatives taken as the reciprocal of the first order rate constants are summarised in Table 7 for both solvent studies. From the result, obviously the triplet lifetime increases with increasing solvent polarity, from acetonitrile to 2-propanol. Since the triplet ³ππ* and ³nπ* states are close in energy in non-polar solvents, vibronic coupling between degenerate states enhances the rate of intersystem crossing to the ground S₀ state, thus reducing the triplet lifetimes. Likewise, in polar solvents the ³nπ* state is destabilised resulting in a decrease in vibronic coupling which reduces the rate of intersystem crossing and increases the triplet lifetime.

Kinetic Studies For 2 Substituted Anthraquinones in Different Media

The kinetic data for all the 2-substituted anthraquinones used in this study are listed in tables 6- 10. The first order decay rate constants increased in the presence of air and oxygen. From the first order decay rates the bimolecular rate constants for the reaction of molecular oxygen with the anthraquinones derivatives studied here were calculated and found vary from 1.2 x 10⁸ mol.dm⁻³ s⁻¹ to 2.5 x 10⁸ mol.dm⁻³ s⁻¹. It is clear from the results that all anthraquinone derivatives are effectively quenched by ground state molecular oxygen. Molecular oxygen (³O₂) is a potent quencher of the

excited states of organic molecules. In the photopolymerisation process, oxygen may interfere with the process by quenching the triplet state of the anthraquinones, thereby preventing the production of primary radicals [13]. If tertiary amines are used as co-initiators, the primary radicals are mainly formed via an exciplex. The formation of the exciplex is not affected by the presence of oxygen. Therefore, the addition of amines to many photoinitiators is an effective means for reducing oxygen inhibition.

Table 6: Transient Absorption Properties of 2BA on Nanosecond Flash Photolysis

	Conditions	λ_{max} (nm)	First Order Rate Decay Rate (s^{-1}) ($k / 10^5$)
2BA	$6.67 \times 10^{-4}\text{M}$ in MeCN (Ar)	370	10.36
	$6.67 \times 10^{-4}\text{M}$ in MeCN (Air)	370	69.70
	$6.67 \times 10^{-4}\text{M}$ in MeCN (O_2)	370	81.60
	$5 \times 10^{-4}\text{M}$ in 2 Propanol (Ar)	370	9.36

Table 7: Transient Absorption Properties of 2CA on Nanosecond Flash Photolysis

	Conditions	λ_{max} (nm)	First Order Rate Decay Rate (s^{-1})($k/10^5$)
2CA	$6.67 \times 10^{-4}\text{M}$ in MeCN (N_2)	370	9.43
	$6.67 \times 10^{-4}\text{M}$ in MeCN (Air)	370	17.41
	$6.67 \times 10^{-4}\text{M}$ in MeCN (O_2)	370	29.5
	$5 \times 10^{-4}\text{M}$ in 2-Propanol (Ar)	370	5.24

Table 8: Transient Absorption Properties of 2EA Nanosecond Flash Photolysis

	Conditions	λ_{max} (nm)	First Order Rate Decay Rate (s^{-1})($k/10^5$)
2EA	$6.67 \times 10^{-4}\text{M}$ in MeCN (N_2)	370	7.160
	$6.67 \times 10^{-4}\text{M}$ in MeCN (Air)	370	11.13
	$6.67 \times 10^{-4}\text{M}$ in MeCN (O_2)	370	35.40
	$5 \times 10^{-4}\text{M}$ in 2 Propanol (Ar)	370	3.52

Table 9: Transient Absorption Properties of 2HA on Nanosecond Flash Photolysis

	Conditions	λ_{max} (nm)	First Order Rate Decay Rate (s^{-1}) ($k/10^5$)
2HA	$6.67 \times 10^{-4}\text{M}$ in MeCN (N_2)	370	3.28
	$6.67 \times 10^{-4}\text{M}$ in MeCN (Air)	370	10.80
	$6.67 \times 10^{-4}\text{M}$ in MeCN (O_2)	370	30.30
	$5 \times 10^{-4}\text{M}$ in 2 Propanol(Ar)	370	3.24

Table 10: Transient Absorption Properties of 2AA on Nanosecond Flash Photolysis

	Conditions	λ_{max} (nm)	First Order Rate Decay Rate (s^{-1}) ($k/10^5$)
2AA	$6.67 \times 10^{-4}\text{M}$ in MeCN (N_2)	370	7.37
	$6.67 \times 10^{-4}\text{M}$ in MeCN (Air)	370	12.51
	$6.67 \times 10^{-4}\text{M}$ in MeCN (O_2)	370	21.32
	$5 \times 10^{-4}\text{M}$ in 2 Propanol (Ar)	370	4.79

Kinetic Study For 2-Substituted Anthraquinones in a Reductive Solvent

Tables 11-15 collectively lists the kinetic data for all anthraquinone derivatives in reductive solvents. The transient species produced are characterised and their behaviour examined in the presence of two reductive solvents, 2 Propanol and a tertiary amine – triethylamine. From the tabulated data it is seen that the addition of increasing the amounts of 2-propanol to acetonitrile solutions to all derivatives, increases the half-life of the triplet but reduces the kinetic order decay rate constants. The derivatives readily form a long lived radical by direct hydrogen atom abstraction from the 2-propanol donor molecule. The growth rate for all derivatives was taken at the same wavelength as the decay rate. This implies that the addition of 2-propanol to acetonitrile obviously produces the growth of another species. The first order growth rate constants of the transients observed are less than 100ns suggesting the formation of a radical ion pair [8]. When triethylamine is added to all five compounds, the same trend happens. The half-life of the triplet is increased but the kinetic order decay rate constants reduced. The amine effect is evidence of the role of a longer species formed via electron transfer to give a radical anion via an exciplex. The activity of the transient species in the presence of this reductive solvent is shown in figures 12-14.

Table 11: Transient Absorption Properties of 2BA in reductive Solvents on Nanosecond Flash Photolysis

	Conditions	λ_{max} (nm)	Half Life (μs)	First Order Rate Decay Rate (s^{-1}) ($k/10^5$)	First Order Growth Rate ($k/10^5$)
2BA	$6.67 \times 10^{-4}\text{M}$ in MeCN (N_2) + $5 \times 10^{-3}\text{M}$ TEA	570	2.42	25.00	
	$6.67 \times 10^{-4}\text{M}$ in MeCN (N_2) + 0.1M TEA	570	2.48	22.50	
	$6.67 \times 10^{-4}\text{M}$ in MeCN (N_2) + 0.1M IPA	380	1.70	18.60	17.64 (380nm)
	$6.67 \times 10^{-4}\text{M}$ in MeCN (N_2) + 0.25M IPA	370	1.98	13.70	15.96 (380nm)
	$6.67 \times 10^{-4}\text{M}$ in MeCN (N_2) + 0.50M IPA	370	2.40	8.40	14.86 (380nm)
	$6.67 \times 10^{-4}\text{M}$ in MeCN (N_2) + 0.75M IPA	370	2.41	3.60	4.29 (380nm)

Table 12: Transient Absorption Properties of 2CA in reductive Solvents on Nanosecond Flash Photolysis

	Conditions	λ_{max} (nm)	Half Life (μs)	First Order Rate Decay Rate (s^{-1}) $k/10^5$	First Order Growth Rate $k/10^5$
2 CA	$6.67 \times 10^{-4}\text{M}$ in MeCN (N_2) + $5 \times 10^{-3}\text{M}$ TEA	560	1.96	28.8	
	$6.67 \times 10^{-4}\text{M}$ in MeCN (N_2) + 0.1M TEA	560	1.87	16.5	
	$6.67 \times 10^{-4}\text{M}$ in MeCN (N_2) + 0.1M IPA	370	1.31	10.31	12.34 (370 nm)
	$6.67 \times 10^{-4}\text{M}$ in MeCN (N_2) + 0.25M IPA	370	1.67	10.00	12.01 (370 nm)
	$6.67 \times 10^{-4}\text{M}$ in MeCN (N_2) + 0.50M IPA	370	1.65	6.71	9.86 (370 nm)
	$6.67 \times 10^{-4}\text{M}$ in MeCN (N_2) + 0.75M IPA	370	1.80	5.30	6.32 (370 nm)

Table 13: Transient Absorption Properties of 2EA in reductive Solvents on Nanosecond Flash Photolysis

	Conditions	λ_{max} (nm)	First Order Rate Decay Rate (s^{-1}) ($k/10^5$)	First Order Growth Rate ($k/10^5$)
2EA	$6.67 \times 10^{-4}\text{M}$ in MeCN (N_2) + $5 \times 10^{-3}\text{M}$ TEA	530	9.87	
	$6.67 \times 10^{-4}\text{M}$ in MeCN (N_2) + 0.1M TEA	530	4.58	
	$6.67 \times 10^{-4}\text{M}$ in MeCN (N_2) + 0.1M IPA	370	8.84	7.65 (370 nm)
	$6.67 \times 10^{-4}\text{M}$ in MeCN (N_2) + 0.25M IPA	370	6.17	5.23 (370 nm)
	$6.67 \times 10^{-4}\text{M}$ in MeCN (N_2) + 0.50M IPA	370	5.31	5.67 (370 nm)
	$6.67 \times 10^{-4}\text{M}$ in MeCN (N_2) + 0.75M IPA	370	4.09	6.14 (370 nm)

Table 14: Transient Absorption Properties of 2HA in reductive Solvents on Nanosecond Flash Photolysis

	Conditions	λ_{max} (nm)	First Order Rate Decay Rate (s^{-1}) ($k/10^5$)	First Order Growth Rate ($k/10^5$)
2 HA	$6.67 \times 10^{-4}\text{M}$ in MeCN (N_2) + $5 \times 10^{-3}\text{M}$ TEA	530	18.00	
	$6.67 \times 10^{-4}\text{M}$ in MeCN (N_2) + 0.1M TEA	530	10.11	
	$6.67 \times 10^{-4}\text{M}$ in MeCN (N_2) + 0.1M IPA	370	6.54	8.90 (370 nm)
	$6.67 \times 10^{-4}\text{M}$ in MeCN (N_2) + 0.25M IPA	370	5.39	8.54 (370 nm)
	$6.67 \times 10^{-4}\text{M}$ in MeCN (N_2) + 0.50M IPA	370	4.11	6.64 (370 nm)
	$6.67 \times 10^{-4}\text{M}$ in MeCN (N_2) + 0.75M IPA	370	4.09	4.18 (370 nm)

Table 15: Transient Absorption Properties of 2AA in reductive Solvents on Nanosecond Flash Photolysis

	Conditions	λ_{\max} (nm)	First Order Rate Decay Rate (s^{-1}) ($k/10^5$)	First Order Growth Rate ($k/10^5$)
2 AA	$6.67 \times 10^{-4}M$ in MeCN (N_2) + $5 \times 10^{-3}M$ TEA	570	9.36	
	$6.67 \times 10^{-4}M$ in MeCN (N_2) + 0.1M TEA	570	7.11	
	$6.67 \times 10^{-4}M$ in MeCN (N_2) + 0.1M IPA	370	11.36	9.78 (370 nm)
	$6.67 \times 10^{-4}M$ in MeCN (N_2) + 0.25M IPA	370	9.01	8.79 (370 nm)
	$6.67 \times 10^{-4}M$ in MeCN (N_2) + 0.50M IPA	370	8.76	10.07 (370 nm)
	$6.67 \times 10^{-4}M$ in MeCN (N_2) + 0.75M IPA	370	7.98	6.89 (370 nm)

From the tabulated data it is seen that the addition of increasing the amounts of 2-propanol to acetonitrile solutions to all derivatives, increases the half-life of the triplet but reduces the kinetic order decay rate constants. The derivatives readily form a long lived radical by direct hydrogen atom abstraction from the 2-propanol donor molecule. The growth rate for all derivatives was taken at the same wavelength as the decay rate. This implies that the addition of 2-propanol to acetonitrile obviously produces the growth of another species. The first order growth rate constants of the transients observed are less than 100ns suggesting the formation of a radical ion pair [8].

When triethylamine is added to all five compounds, the same trend happens. The half-life of the triplet is increased but the kinetic order decay rate constants reduced. The amine effect is evidence of the

role of a longer species formed via electron transfer to give a radical anion via an exciplex. The activity of the transient species in the presence of this reductive solvent is shown in figures 12-14.

Figure 12

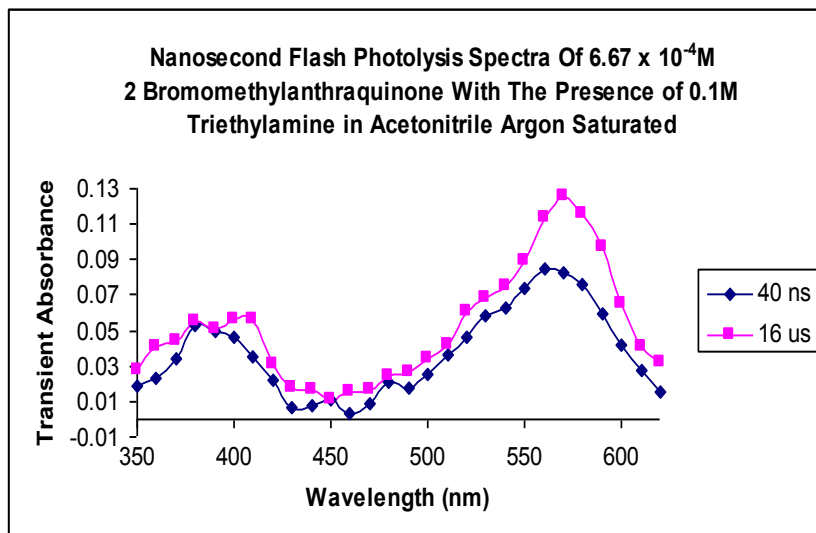


Figure 13

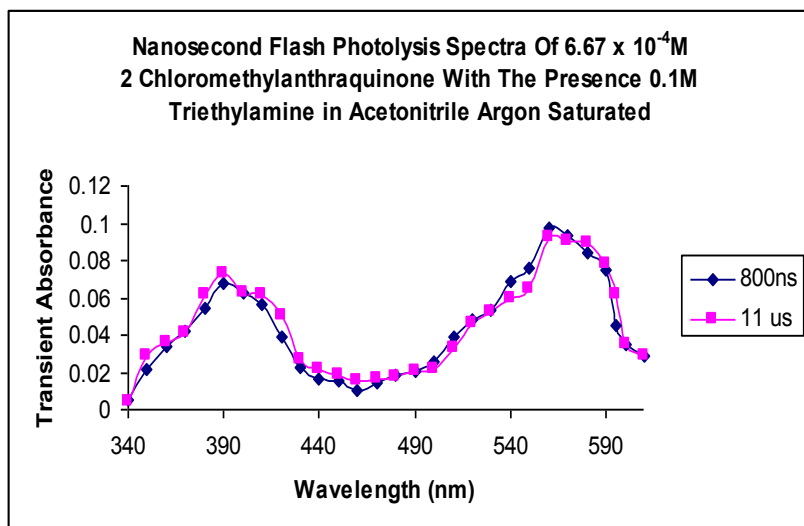
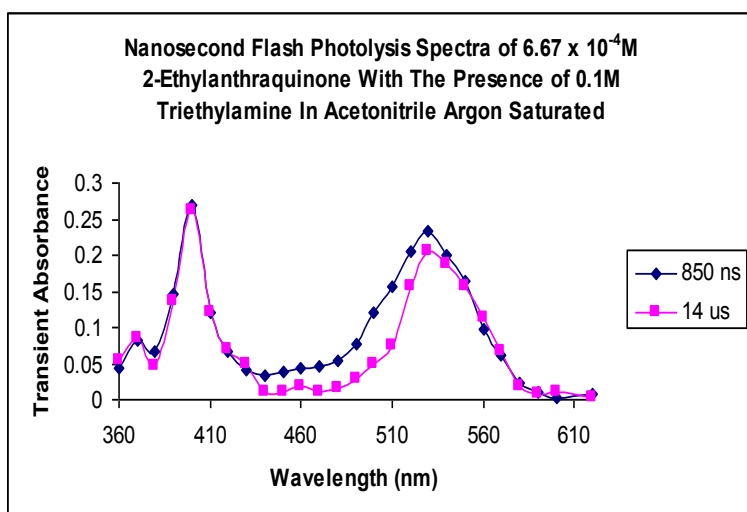
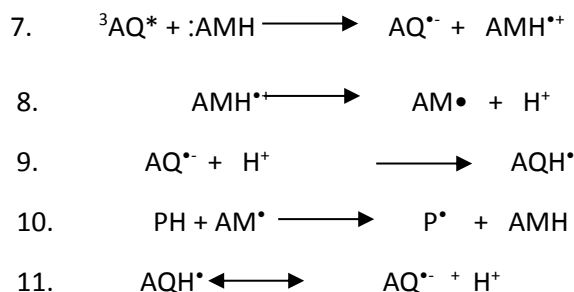


Figure 14



All the figures show a strong residual absorption at long time delays would thus indicate the formation of long lived radical species. The presence of amine enables an electron transfer process to occur regardless of the nature of the lowest excited triplet state. The other evidence for the matter could be seen in the oscilloscope kinetic traces showing the decay of quinone at 400 nm and the formation or growth of a radical anion at 540 nm as seen in the spectra.

The data in this nanosecond flash photolysis study leads to the conclusion that a quinone that has been excited into a triplet state ($^3\text{AQ}^*$) subsequently forms a radical anion ($\text{AQ}^{\bullet-}$) and alkylamino radical (AM^\bullet) with an amine molecule ($:\text{AMH}$). The radical anion is thus capable of abstracting a proton to give the semi-anthraquinone radical (AQH^\bullet) and the alkylamino radical can also abstract a hydrogen atom from the polymer (PH). Radical anions ($\text{AQ}^{\bullet-}$) can exist in equilibrium with the semi-anthraquinone radical (AQH^\bullet). This can form a reactive ion-pair:



Energy Transfer and Molar Absorption Coefficient.

Intermolecular exchange of energy between two species is another important photochemical step. It is important since the transfer represents a process whereby potentially reactive species can be formed. Both species involved are named 'acceptor' and 'donor' respectively. In electronic energy transfer, an excited donor molecule D^* is deactivated to its ground state D , while transferring its electronic excitation energy to an acceptor molecule A . In the present work, the energy transfer reaction is between the triplet state of 2 substituted anthraquinones ($^3A^*$) and the ground state of Fenbufen giving ($^3Fen^*$) :



The molar absorption coefficients of the triplet states of the 2 substituted anthraquinone derivatives in acetonitrile solution were estimated by monitoring the energy transfer reaction between the two species above. In this work, $6.67 \times 10^{-4}M$ 2 substituted anthraquinone derivative solutions containing $1.8 \times 10^{-4}M$ Fenbufen in acetonitrile were given a laser pulse.

Under these conditions, all the light energy absorbed was taken up by the 2 substituted anthraquinone derivatives (A). The triplet state of the A (3A) was thus produced within the laser pulse lifetime, with an absorption maximum at around 370 nm, followed by the formation of a new absorption band at 420nm which is attributed to the triplet of of Fenbufen [14]. The spectrum of triplet-triplet energy transfer between the (2HA) and (2 AA) with fenbufen on a different time scale from the nanosecond flash photolysis, are shown in figures 15 and 16.

Figure 15

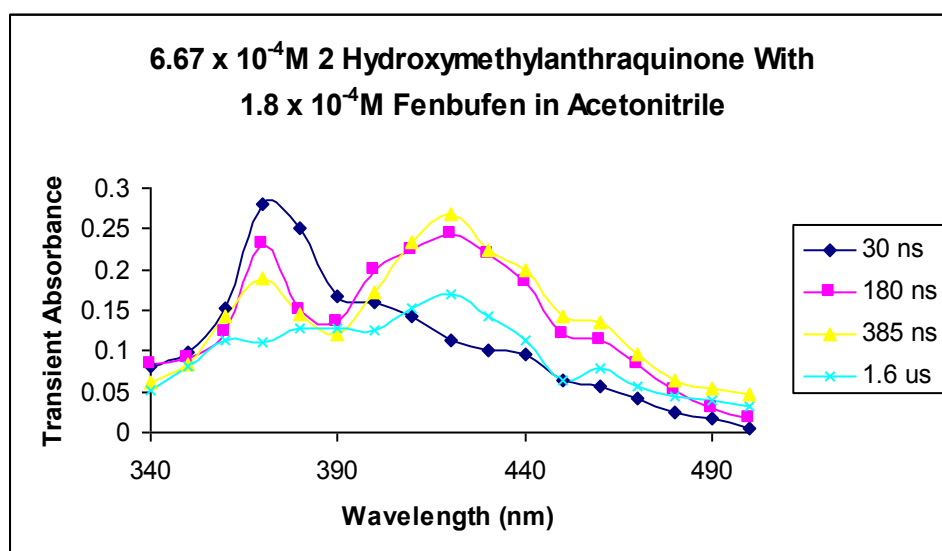
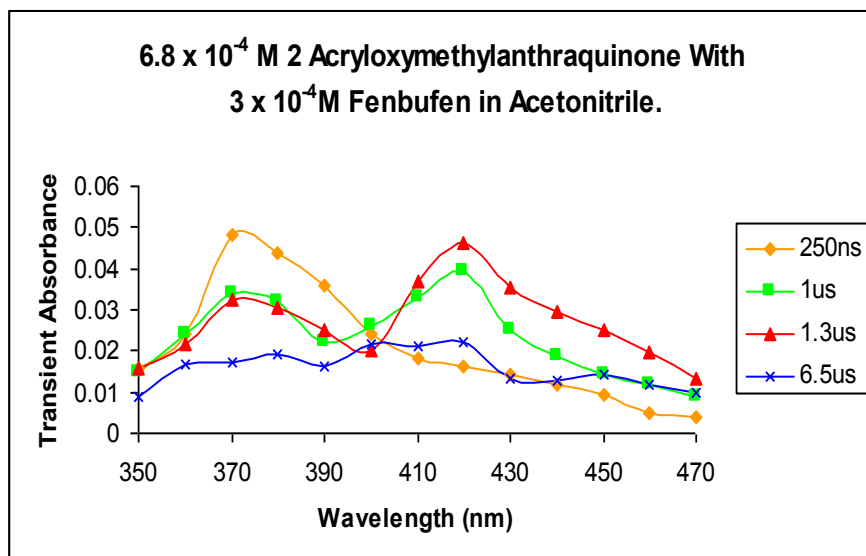
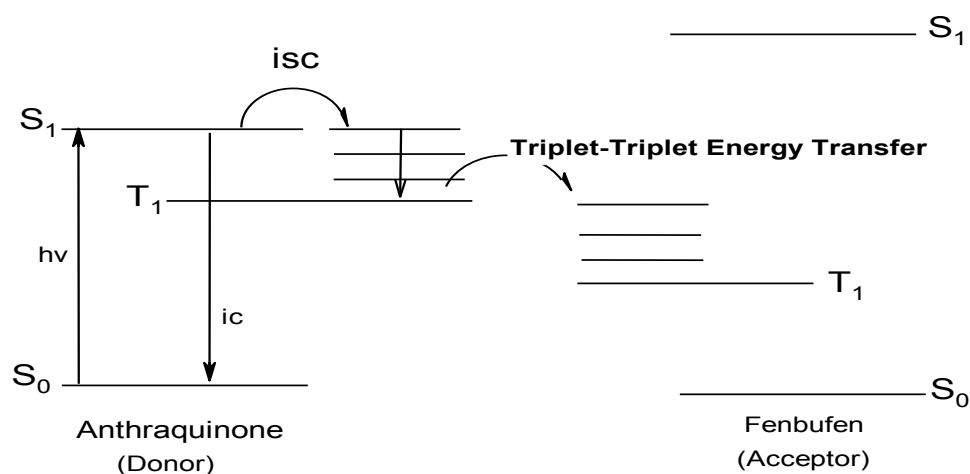


Figure 16



It is clear from the spectra that there are two absorption maxima at different wavelengths. In the beginning of the reaction, at 370 nm the triplets of 2HA and 2AA are produced respectively. The mixture of both triplets exists in acetonitrile at $t = 180\text{ns}$ and $t = 1\mu\text{s}$ respectively. Moving to a longer time scale, the triplets of anthraquinone derivatives are mostly quenched to produce triplets for fenbufen via energy transfer between the two species. A longer live triplet is seen in figure 15 compared to figure 16 as in the latter figure, most of the triplet has decayed at $t = 1.6\mu\text{s}$. Triplet-triplet energy transfer can occur when the relative energies of the lowest excited states of the donor and acceptor are as in figure 17.

Figure 17: Favourable arrangement of anthraquinone-fenbufen energy levels for triplet-triplet energy transfer



Transfer from the S_1 state of 2- substituted anthraquinone derivatives to the S_1 and T_1 states of fenbufen are respectively energy- and spin forbidden and hence are inefficient processes as compared to the T_1 to T_1 transfer which is both energy- and spin allowed. Similarly, transfer from the T_1 state of 2 substituted anthraquinone derivatives to the S_1 state of Fenbufen will be highly inefficient since this process is both energy- and spin forbidden. Thus, to evaluate the molar absorption efficiency, initially the fraction of anthraquinone triplet state converted to the fenbufen was calculated, using the equation (1) and data shown in Table 16.

$$(eq. 1) \quad F = (K_1 - K_0) / K_1$$

Where:

K_1 = First Order Decay Of 2-Substituted Anthraquinone Derivatives with Fenbufen

K_0 = First Order Decay of 2-Substituted Anthraquinone Derivatives without Fenbufen

Table 16: Fraction and Percentage of 2 Substituted Anthraquinones Triplet State Quenched into Fenbufen Triplet

Anthraquinone	Fraction (F)	Percentage (%)
2 BA	0.776	77.6
2 CA	0.889	88.9
2 EA	0.927	92.7
2 HA	0.921	92.1
2 AA	0.951	95.1

The molar absorption coefficients of the triplet states of 2-substituted anthraquinone derivatives, were then calculated using the equation below:

$$(Eq. 2) \quad \frac{F A_{A^*}}{A_{Fe^*}} = \frac{\epsilon_{A^*}}{\epsilon_{Fe^*}}$$

Here the A values refer to the absorbances of the triplet states of the anthraquinone at the beginning of the reaction at their respective maxima and of fenbufen triplet state at the end of the reaction at 420nm. The molar absorption coefficient of fenbufen triplet at 420nm is taken as 30,000 dm³ mol⁻¹

cm⁻¹ [14]. The molar absorption coefficients can be used to calculate the quantum yields for intersystem crossing for the anthraquinones (Φ_{isc}) in acetonitrile solution. This is achieved by giving laser pulses to solutions of benzophenone and comparing the maximum absorbance observed at 520 nm, attributable to the triplet state of the benzophenone, with that of the absorbance observed at 370 nm after giving the identical laser pulse to solutions of the anthraquinone. The quantum yield of the 2-substituted anthraquinone triplet states are then calculated of the following equation:

$$(Eq. 3) \quad \frac{A_{BZ^* (355)}}{A_{A^* (355)}} = \frac{\epsilon_{BZ^* (355)} \Phi_{isc(BZ)}}{\epsilon_{A^* (355)} \Phi_{isc(A)}}$$

Where the absorbance, A and molar absorption coefficients, ϵ , are the corresponding triplets of benzophenone and 2-substituted anthraquinones. The quantum yields for intersystem crossing of benzophenone is taken to be 1.0, while the molar coefficient of the triplet state benzophenone was found to be 6500 dm³ mol⁻¹ cm⁻¹. The triplet-triplet molar absorption coefficients and the quantum yield for intersystem crossing is given in Table 17.

Table 17: Triplet-triplet molar absorption coefficients (ϵ) and quantum yield of intersystem crossing (Φ_{isc}) of 2-substituted anthraquinone derivatives in acetonitrile (Absorbance = 0.5 at 355 nm (at λ_{max}))

Compound	$\epsilon / \text{dm}_3 \text{ mol}^{-1} \text{ cm}^{-1}$	Φ_{isc}
Benzophenone	6,640	1.00
2BA	8,075	0.80
2CA	8,412	0.77
2EA	15,100	0.43
2HA	13,067	0.50
2AA	14,604	0.46

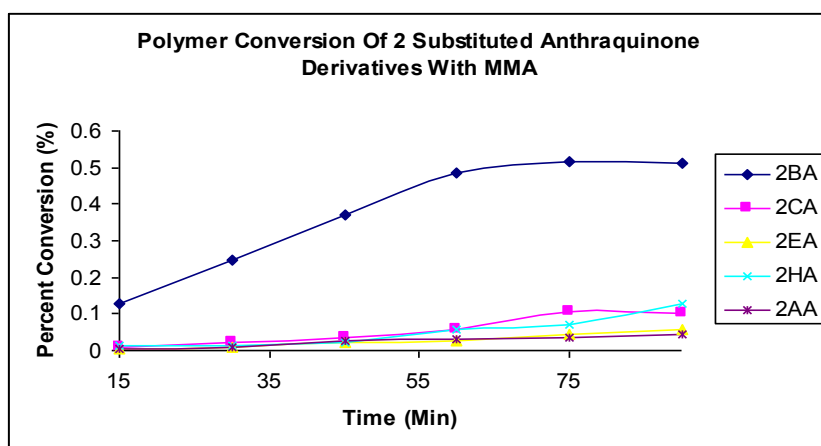
Triplet-triplet energy transfer is a way to enhance the population of the triplet. The higher quantum yield in benzophenone arises because of the greater efficiency of the $S_1 \rightarrow T_1$ transition. Between the anthraquinones, the highest quantum yield is 2BA, suggesting the energy transfer from 2BA to fenbufen is rapid, and that once 2BA triplet molecules are formed energy is transferred fast to

fenbufen to give the fenbufen triplet state. Lower quantum yield in 2AA, suggest the production of triplet for this compound is also relatively low.

Photopolymerisation Study

The initial rates of polymerisation for 2-substituted anthraquinone were calculated with methyl methacrylate monomer. Figure18 illustrates the conversion curves for the polymerisation with relatively low conversion of the monomer, with the exception for 2BA.

Figure 18



The rates of polymerisation (R_p) for all anthraquinone derivatives are calculated in Table 18. The rates were also calculated in the presence of a tertiary amine to determine its effect on the rate of photopolymerisation.

Table 18: Rates of Polymerisation For 2-Substituted Anthraquinones with and Without Amine as the Co-Synergist

Compound	Absence of Amine (R_p)	Presence of Amine (R_p)
2 BA	2.52×10^{-4}	2.03×10^{-4}
2 CA	4.67×10^{-4}	4.17×10^{-4}
2 EA	3.27×10^{-3}	3.10×10^{-3}
2 HA	3.01×10^{-3}	2.13×10^{-3}
2 AA	4.33×10^{-3}	4.15×10^{-3}

In the presence of the tertiary amine, the rate of polymerisation for all compounds is reduced. This observation can be explained by the observation that all the derivatives are identified as having an $n-\pi^*$ lowest excited triplet state. The excited states of these derivatives are highly efficient at producing reactive radicals without a co-initiator. 2AA showed the highest rate in the absence of amine as the compound is the ester type molecule that is sufficiently active to abstract a hydrogen atom from the environment. The result indicates that the photopolymerisation activity of these compounds are independent of the configuration of the lowest excited triplet state.

Pendulum Hardness

Reactive diluents are commonly used to reduce the viscosity of the resins. The addition of multifunctional monomers in the formulation will also improve crosslinking. In this work two types of diluents used were TPGA and GPTA and they were added to the resin to study the hardness properties. TPGA and GPTA are often used in these systems due to their high reactivity, good viscosity and reasonable cost. Problems arise in the work, as most of the photoinitiators have a difficult solubility in the formulation. Many methods were undertaken to dilute the photoinitiators before using it in the formulation. Among the ways, was by diluting them initially in a soluble solvent. Figures 19 and 20 show the pendulum hardness values with the different curing time of 50/50 w/w mixture of oligomers epoxy acrylate, Actilane 320 with TPGDA and GPTA respectively at 6° of amplitude.

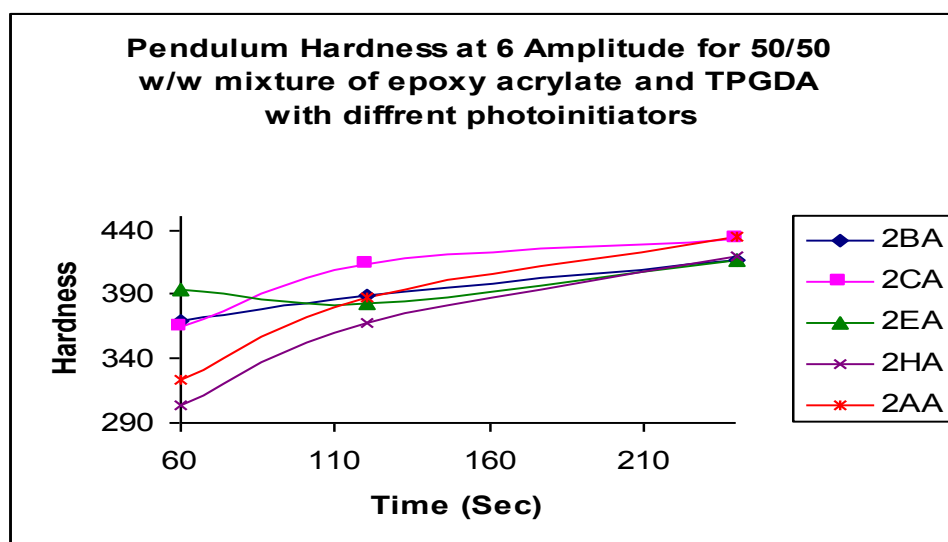
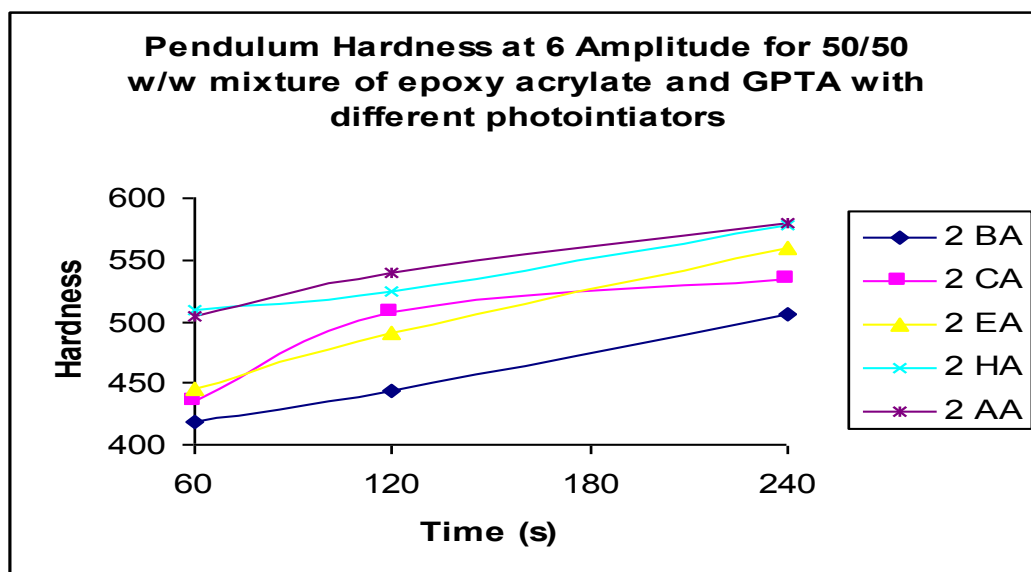


Figure 19

Figure 20



As expected the higher functionality trifunctional monomer, GPTA, showed a higher crosslinking ability than the difunctional monomer TPGDA. Formulations containing GPTA are also harder than TPGDA for the same reason. The results obtained confirm that a better surface cure can be obtained in combined systems resin/acrylate when a higher functionality monomer is used.

From a comparison of the initiators it is clearly shown that in the mixture of epoxy resin and TPGA, 2BA shows the highest efficiency while the other photoinitiators are having a similar trend and level of efficiency. Contrary to this in figure 20, curing with an epoxy resin and GPTA mixture, 2BA showed the lowest efficiency. Among all photoinitiators, 2 BA has the lowest solubility in the mixture. It is acceptable therefore, that this effect contributes to the lower efficiency than the other initiators. However, the result in figure 19 does not support this effect.

In this case this range of 2-substituted anthraquinones clearly exhibit differing photoactivities and excited state properties. All form the semianthraquinone radical which in basic media can also form directly or indirectly the radical anion species. Both can act as photoinitiators of polymerisation. The insolubility data in commercial acrylates is inconclusive here whereas the methyl methacrylate data displays some correlation with structure and activity. Of all the molecules the 2-Bromo derivative is the most active and this is well supported by its high triplet yield formed by rapid intersystem crossing. This is then followed by the excited state data for the 2-Cl derivative. The 2-acryloxymethyl derivative on the other hand exhibits very low activity and this is displayed by its low triplet activity and possibility of a competitive scission or photolysis reaction giving rise to unreactive aromatic radicals.

CONCLUSIONS

This study alongside our previous investigations was directed toward continued efforts improve photopolymerizable initiators for UV radiation coating technology-especially reactive types for non-extraction and inter-relate this with their excited state properties. The substituent groups attached in the 2-position have a profound effect on the photoactive behaviour of the anthraquinone molecule. The nature of the lowest excited states depends on electron donation to the conjugated ring system, which is in turn dependant on the structure of the substituent group in the two (2) position. The novel synthesis and experiments of 2AA has provided an interesting scope of knowledge in this regard.

The type of electronic transitions accruing upon the absorption of light are established via UV/luminescence spectroscopy. All the anthraquinone derivatives in this work are electron donating. Four derivatives (2BA, 2CA, 2EA and 2HA) with halo functionality and the novel anthraquinone (2AA) with an ester functionality possess a lowest triplet excited state with an $n-\pi^*$ configuration. Initially the results showed all the compounds possessed a lowest singlet state with $\pi-\pi^*$ character with some mixed $n-\pi^*$ influence. However, the low value of the extinction coefficient, ϵ , indicates that all compounds have an $n-\pi^*$ transition and that the S_1 state is ($n\pi^*$) in character.

Luminescence studies in this work provided consistent evidence in support of the proposed state for all the anthraquinones. Rapid deactivation of the lowest excited singlet $n\pi^*$ state by efficient intersystem crossing (ISC) to the lowest lying excited triplet state is observed from the low fluorescence quantum yields for all compounds. Strong phosphorescence emission occurs from the excited $^3n-\pi^*$ to the ground state. Among the 5 compounds, 2BA and 2CA exhibits the highest quantum yield but with a reduce lifetime. This is associated with the presence of heavy atoms (Br, Cl) enhancing the rate of intersystem crossing through spin-orbit coupling.

From microsecond flash photolysis it can be concluded that the anthraquinone derivatives undergo photoreduction via hydrogen atom abstraction to produce active radical anion species. The addition of triethylamine to the system has the most significant effect on the absorbance in region 450-550 nm which increases due to the existence of a radical anion. The effect of the configuration of the lowest excited triplet states can be seen in the studies where the anthraquinone molecules are in a photoreduction environment. The molecules possessing $n-\pi^*$ lowest triplet state can be efficiently reduced by both amine and alcohol donors. The interesting feature of the nanosecond flash photolysis data is that the singlet-triplet absorption maxima for all anthraquinones are in the range of 320-500

nm that belongs to the triplet $^3n-\pi^*$ group. The absorption maxima of the substituted anthraquinone is red shifted bathochromically on changing the solvent from acetonitrile to 2-propanol. The mechanism of abstracting a hydrogen atom from 2-propanol occurs via the triplet state to the parent anthraquinone leading eventually to the formation of its radical anion. The most long-lived radical among the anthraquinones is 2AA which has an ester link. This agrees with previous studies [8] that de-esterification takes place at ring positing to give a long-lived, stabilised aromatic radical.

First order rate decays for the triplet state increase in the presence of oxygen, showing that all anthraquinones are efficiently quenched by oxygen. In the presence of increasing amounts of 2-propanol to the acetonitrile solution for all derivatives, the kinetic order decay decreases while the half-life, increases. This confirms the existence of the growth of another species. All derivatives interact strongly with triethylamine to form an exciplex via electron transfer. Strong absorption can be seen at long time delays which indicates the formation of long lived radical species. Through the energy transfer experiment using fenbufen with all derivatives, triplet molar coefficients, ϵ , have been calculated and are found to be higher than benzophenone which is used as a standard. All the compounds are observed to possess relative quantum yields of intersystem crossing ($\Phi_{isc} > 0.6$) but their values are lower than that observed for benzophenone with the side chain substituents having no significant effect on the rate and intersystem crossing efficiency.

The polymerisation study showed an interesting observation in the rate of polymerisation in the presence of an amine. The rate of polymerisation is reduced. It showed that in the presence of the tertiary amine their polymerisation efficiency decreases. This is because molecules that possess an $n-\pi^*$ excited triplet configuration can react predominantly via direct hydrogen atom abstraction. The surface cure of commercial prepolymer/diluent monomer systems indicates that 2BA induces a different hardness property in different formulae although here the effect in the resins may well be due to solubility and cage effects on radical formation. For the more soluble MMA monomer the 2-BA exhibits the most reactivity due to its higher rate of triplet formation and quantum yield of intersystem crossing.

ACKNOWLEDGEMENTS

The authors thank the University of Sains Malaysia for funding Hazira Mazah.

REFERENCES

1. N.S. Allen, P. Bentley and J.F. Mckellar, J. Photochem., 5, (1976) 225-231.
2. N.S. Allen and J.F Mckellar, J. Photochem., 5, (1976) 317-321.

3. N.S. Allen, J.P. Hurley, M. Edge, G. Follows, I. Weddell and F. Catalina, *J. Photochem. & Photobiol, Chem. Ed.*, 71, (1993) 109-114.
4. N.S. Allen, G. Pullen, M. Shah, M. Edge, I. Weddell, R. Swart and F. Catalina, *J. Photochem. & Photobiol Part A: Chem. Ed.*, 91, (1995) 73-79.
5. N.S. Allen, G. Pullen, M. Shah, M. Edge, I. Weddell, R. Swart and F. Catalina, *Polymer*, 36, (1995) 4665-4674.
6. M. Shah, N.S. Allen, M. Edge, S. Navaratnam and F. Catalina, *J. Appl. Polym. Sci.*, 62, (1996) 319-340.
7. N.S. Allen, G. Pullen, M. Edge, I. Weddell, R. Swart and F. Catalina, *J. Photochem. & Photobiol. Part A: Chem. Ed.*, 109, (1997) 71-75.
8. F. Catalina, C. Peinado, M. Blanco, T. Corrales and N.S. Allen, *Polymer*, 42, (2001), 141-146.
9. S. Navaratnam, (2004) Photochemical and photophysical methods used in the study of drug phototoxicity. In *Photostability of Drugs & Drug Formulations* (Edited by H. H. Tonnesen), CRC Press, Boca Raton, pp. 255–284.
10. R.M. Hochstrasser and C.A. Marzacco in E.C. Lim (editor). *Int. Conf. on Molecular Luminescence*, Benjamin Pub., N.Y., (1969), 631.
11. B.E. Hulme, E.J. land and G.O. Phillips, *J. Chem. Soc., Farad. Trans., I*, 68 (1972), 2003.
12. K. Hamanoue, T. Nakayama, Y. Yamamoto, K. Sawada, Y. Yuhara and H. Teranishi, *Bull. Chem. Soc., Jpn.*, 61, (1988), 1121-1129.
13. K.K. Dietlicker in *Chemistry and Technology of UV and EB Formulations for Coatings, Inks and Paints*, Vol. III, "Photoinitiators for Free radical and Cationic Polymerisation", Ed. P.K.T. Oldring, SITA Technology Ltd., (1991).
14. S. Navaratnam and S.A. Jones *PhotochemPhotobiol A* 132 (2000) 175-180.